Quantum interference between multiple impurities in anisotropic superconductors

Brian Møller Andersen and Per Hedegård
Ørsted Laboratory, Niels Bohr Institute for APG, Universitetsparken 5, DK-2100 Copenhagen Ø, Denmark
(Received 14 January 2003; published 14 May 2003)

We perform a numerical study of the quantum interference between impurities in *d*-wave superconductors within a potential scattering formalism that easily applies to multiple impurities. The evolution of the low-energy local density of states for both magnetic and nonmagnetic point scatterers is studied as a function of the spatial configuration of the impurities. Further we discuss the influence of a subdominant bulk superconducting order parameters on the interference pattern from multiple impurities.

DOI: 10.1103/PhysRevB.67.172505 PACS number(s): 74.25.Jb, 72.10.Fk, 71.55.−i

The past few years have proved the importance of experimental techniques which can directly test the wealth of information associated with modifications of the local density of states (LDOS) around impurities, grain boundaries, and vortices in strongly correlated electron systems. In particular, scanning-tunneling microscopy (STM) measurements have provided detailed LDOS images around single nonmagnetic[1,2] (Zn) and magnetic[3] (Ni) impurities on the surface of the high-temperature superconductor $Bi_2Sr_2CaCuO_{4+\delta}$ (BSCCO).

For conventional superconductors Yu and Shiba[4] showed that as a result of the interaction between a magnetic impurity and the spin density of the conduction electrons, a bound state located around the magnetic impurity is formed inside the gap in the strong-scattering (unitary) limit. For anisotropic superconductors a number of authors generalized the Yu-Shiba approach to study the LDOS around single impurities.[5] It was found, for instance, that for a single nonmagnetic impurity there is only a virtual bound (or resonant) state due to the existence of the low-energy nodal quasiparticles. The one-impurity problem was recently reviewed by several authors.[6,7]

Recently Hoffman *et al.*[8] measured the energy dependence of the Fourier-transformed LDOS images on the surface of optimally doped BSCCO below T_c. The dispersive features were explained from the point of elastic quasiparticle interference resulting from a single *weak*, nonmagnetic impurity.[9] This gives credence that a scattering potential picture can yield valuable predictions in the superconducting state of these materials. Evidence for quantum interference between *strong* scatterers has been observed in the CuO chains of $YBa_2Cu_3O_{6+x}$ by Derro *et al.*[10] Future experimental ability to control the position of the impurities on the surface of a superconductor and perform detailed STM measurements around multiple impurity configurations motivates further theoretical studies of the resulting quantum interference.

Previous calculations have studied the formation of bonding and antibonding states around two magnetic impurities in *s*-wave superconductors.[11,12] For *d*-wave superconductors it was found that the interference effects between two nonmagnetic unitary scatterers depends crucially on the distance and orientation of the impurities.[6,7,13] The orientational dependence arises from the anisotropic gap function and provides an alternative method to identify the symmetry of the superconducting gap. Several authors[5,14] have previously suggested similar ideas in the case of one impurity.

In this paper we study multiple impurity effects by exactly inverting the Gorkov-Dyson equation. In particular, we discuss the effect of quantum interference between (i) nonmagnetic impurities in the strong-scattering limit, (ii) nonmagnetic impurities in the case of induced subdominant superconducting order parameters, and (iii) magnetic and nonmagnetic impurities. All the calculations are performed within a quasiparticle scattering framework with classical impurities.[4,14] The main purpose is to use quantum interference to obtain results that motivate further testing on this approach and to illustrate the strong sensitivity of the LDOS on the positions of the impurities.

The Green's function $\hat{G}^{(0)}(\mathbf{k},\omega)$ for the unperturbed *d*-wave superconductor is given in Nambu space by

$$\hat{G}^{(0)}(\mathbf{k},\omega)=[i\omega_n\hat{\tau}_0-\xi(\mathbf{k})\hat{\tau}_3-\Delta(\mathbf{k})\hat{\tau}_+-\Delta^*(\mathbf{k})\hat{\tau}_-]^{-1}, \tag{1}$$

where $\hat{\tau}_\nu$ denotes the Pauli matrices in Nambu space, $\hat{\tau}_0$ being the 2×2 identity matrix and $\hat{\tau}_\pm=\hat{\tau}_1\pm\hat{\tau}_2$. For a system with $d_{x^2-y^2}$-wave pairing, $\Delta(\mathbf{k})=\Delta_0/2[\cos(k_x)-\cos(k_y)]$. Below, $\Delta_0=25$ meV and the lattice constant a_0 is set to unity. In this brief report we use a normal-state quasiparticle energy $\xi(\mathbf{k})$ relevant for BSCCO around optimal doping (14%),

$$\xi(\mathbf{k})=-2t[\cos(k_x)+\cos(k_y)]-4t'\cos(k_x)\cos(k_y)-\mu, \tag{2}$$

with $t=300$ meV, $t'=-0.4t$, and $\mu=-1.18t$. Here t (t') refers to the nearest- (next-nearest-) neighbor hopping integral and μ is the chemical potential.

We model the presence of scalar and magnetic impurities in the system by the following δ-function interactions:

$$\hat{H}^{int}=\sum_i\ [(V_i^S+V_i^M)\hat{c}_{i\uparrow}^\dagger\hat{c}_{i\uparrow}+(V_i^S-V_i^M)\hat{c}_{i\downarrow}^\dagger\hat{c}_{i\downarrow}]. \tag{3}$$

Here i denotes the set of lattice sites containing magnetic and/or scalar impurities, and V_i^M (V_i^S) is the strength of the corresponding effective potential. We consider only the z component of the magnetic impurity interaction and ignore spin-flip scattering.

For a single nonmagnetic impurity at the origin it is well known that the scattering modifies the Green's function by

$$\delta G_{11}(\mathbf{r},i\omega_n)=\frac{[G_{11}^{(0)}(\mathbf{r},i\omega_n)]^2}{\frac{1}{V^S}-G_{11}^{(0)}(0,i\omega_n)}-\frac{[G_{12}^{(0)}(\mathbf{r},i\omega_n)]^2}{\frac{1}{V^S}-G_{11}^{(0)}(0,-i\omega_n)}. \tag{4}$$

Here r is the distance to the origin, and $G_{\alpha\beta}$ refers to the $\alpha\beta$th entry of the 2×2 Nambu subspace.

Naturally one can derive equivalent expressions for the LDOS modulations around several impurities. However, for a numerical study of the evolution of the LDOS for multiple impurities positioned at arbitrary lattice sites, we find it is easier to invert directly the real-space Gorkov-Dyson equation. The full Green's function $\hat{G}(\mathbf{r},\omega)$ is then obtained by solving the equation

$$\underline{\underline{\hat{G}}}(\omega)=\underline{\underline{\hat{G}}}^{(0)}(\omega)[\underline{\underline{\hat{I}}}-\underline{\underline{\hat{H}}}^{int}\underline{\underline{\hat{G}}}^{(0)}(\omega)]^{-1}, \tag{5}$$

where the double lines indicate that the elements of this equation are matrices written in real and Nambu space. The size of these matrices depends on the number of impurities and the dimension of the Nambu space. We have previously utilized this method to study the electronic structure around vortices that operate as pinning centers of surrounding stripes.[15] We perform the two-dimensional Fourier transform of the clean Green's function $\hat{G}^{(0)}(\mathbf{k},\omega)$ numerically by dividing the first Brillioun zone into a 1400×1400 lattice and introducing a quasi-particle energy broadening of $\delta=0.5$ meV with δ defined from $i\omega_n\rightarrow\omega+i\delta$.

The differential tunneling conductance is proportional to the LDOS $\rho(\mathbf{r},\omega)$, which in turn is determined from

$$\rho(\mathbf{r},\omega)=-\frac{1}{\pi}\mathrm{Im}[G_{11}(\mathbf{r},\omega)+G_{22}(\mathbf{r},-\omega)]. \tag{6}$$

In the following we model the nonmagnetic unitary scatterers with a potential $V^S=700$ meV, which gives rise to resonance energies around ±1.5 meV in agreement with experiment.[2] [This is seen from the holelike resonance evident in the bottom LDOS scan in Fig. 5(a) below. For a single impurity only one of the two resonances evident from Eq. (4) has weight on the impurity site since the anomalous part of the Green's function, $G_{12}(r,\omega)$, vanishes at $r=0$ due to the symmetry of the d-wave gap.]

For interference between two nonmagnetic unitary impurities Morr and Stavropoulos *et al.*[6] found strong variations in the LDOS as the distance between the impurities R is varied along one of the crystal axes. The single-impurity spectrum was obtained when R exceeds approximately $10a_0$. However, as expected for a $d_{x^2-y^2}$-wave superconductor, this length scale is much larger along the nodal directions. This is seen in Fig. 1. Here the density of states is measured above one of the impurities fixed at the origin while the other is moved away along the nodal [Fig. 1(a) or anti-nodal [Fig. 1(b)] direction. The single-impurity LDOS is obtained for R well above $100a_0$. Thus only for impurity concentrations below 0.1% does the LDOS correspond to the expected result from a single strong nonmagnetic impurity. For weaker scatterers the decay length will be considerably reduced.

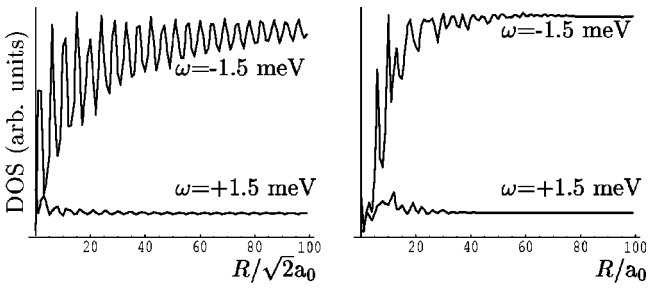

FIG. 1. DOS at (0,0) and at the single-impurity resonance energy ±1.5 meV as a function of distance between the two nonmagnetic impurities separated along the (a) nodal direction and (b) antinodal direction. The y-axis scale is identical for the two figures.

For quantum interference between multiple fixed nonmagnetic unitary scatterers Fig. 2 shows the LDOS as the STM tip is scanned along a crystal axis on which the impurities are positioned. In general the resonances are split by the proximity of other impurities, and the number of resonances is directly proportional to the number of interfering impurities. However, locally the density of states may be strongly influenced by destructive interference. For instance, for the two impurities [Figs. 2(a) and 2(c)] sharp resonances exist only when $R=2a_0$, as is evident from Fig. 2(c). When a third impurity is added at $(-2,0)$ these resonances appear to broaden and shift to higher energies, Fig. 2(d). Contrary to this, Figs. 2(a) and 2(b) show that the addition of a third impurity has only a minor effect when $R=a_0$.

The case of three nonmagnetic impurities is studied further in Fig. 3, which shows the evolution of the LDOS at (0,0) as a function of the distance to a third impurity along the nodal [Figs. 3(b) and 3(d)] anti-nodal [Figs. 3(a) and 3(c)] directions. The case without the third impurity corresponds to the topmost LDOS in Figs. 2(a) and 2(c).

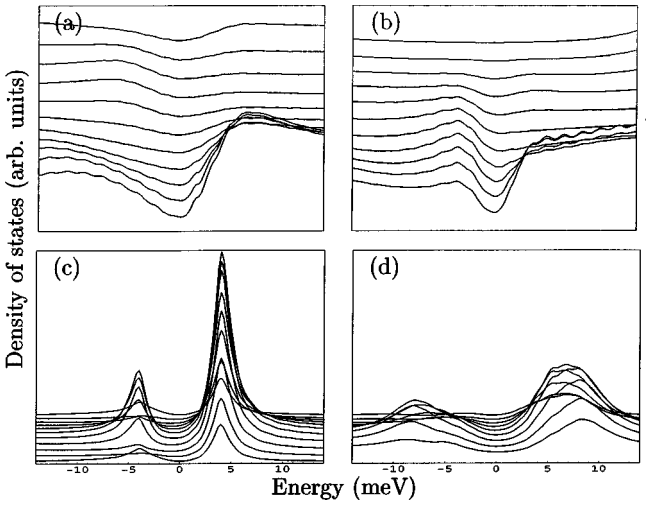

FIG. 2. Low bias STM scans along the horizontal axis in steps of $a_0/5$ from (0,0) (top line) to (2,0) (bottom line). The scans are offset for clarity. In (a) and (c) there are two nonmagnetic impurities fixed at (a) (0,0) and (1,0); (c) (0,0) and (2,0). In (b) and (d) there are three nonmagnetic impurities each at (b) $(-1,0)$, (0,0), and (1,0); (d) $(-2,0)$, (0,0), and (2,0).

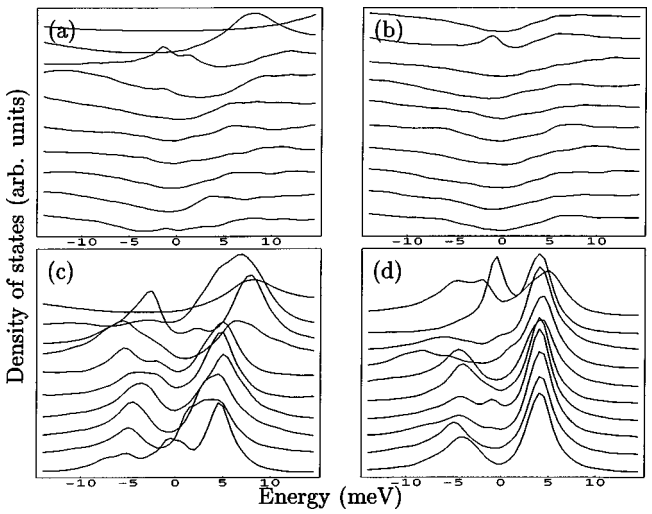

FIG. 3. LDOS at (0,0) as a function of distance to a third impurity along the antinodal (a) and (c) or nodal (b) and (d) direction. The two fixed impurities are positioned at (a) and (b): $(-1,0)$ and (0,0); (c) and (d): $(-2,0)$ and (0,0). In (a) and (c) the third impurity is positioned at (top to bottom) (1,0), (2,0), . . . ,(10,0). In (b) and (d) the third impurity is positioned at (top to bottom) (1,1),(2,2), . . . ,(10,10).

As in the case of two nonmagnetic impurities[6,7] there are very strong variations in the final LDOS; the number of apparent resonances, their width, and resonance energy depend crucially on the positions of the three impurities. The small modulations added by the third impurity seen in Figs. 3(a) and 3(b) agree with the destructive interference evident from the corresponding cases seen in Figs. 2(a) and 2(b). Contrary to this, large modulations are again seen when increasing the distance between the two fixed impurities by a single lattice constant, Figs. 3(c) and 3(d).

Recently Zhu *et al.*[7] suggested a careful study of the two-impurity problem to extract information of the bulk Green's function of the clean system. In the following we show how the quantum interference between unitary scatterers is strongly affected by the induction of a small subdominant superconducting order parameter. Thus one may utilize the quantum interference between several impurities as an alternative method to detect a small subdominant order parameter.

For instance, tuning through a quantum phase transition from a $d_{x^2-y^2}$ to a $d_{x^2-y^2}+id_{xy}$ superconductor at a critical doping level,[16] magnetic impurity concentration,[17] or magnetic-field strength,[18] a small d_{xy} order could *qualitatively* alter the interference pattern. For $\Delta_{xy}(\mathbf{k}) = \Delta_{xy}^0 \sin(k_x)\sin(k_y)$ with $\Delta_{xy}^0 = 5.0$ meV, we compare in Fig. 4 the LDOS at physically realizable impurity positions to the case with $\Delta_{xy}^0 = 0$.

Also we show the difference between $d+id$ and $d+is$ pairing symmetry for these impurity configurations. For most spatial configurations the secondary pairing (id or is) leads to a sharpening of the resonances, but at particular positions there is a qualitative difference, as shown in Fig. 4. For instance, the induction of $d+id$ pairing [Fig. 4(b)] can result in three apparent resonances contrary to the ground state

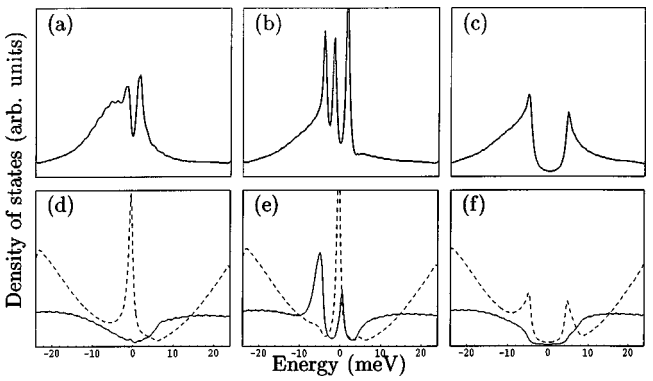

FIG. 4. Top row: DOS at (0,0) for two nonmagnetic impurities at (0,0) and (2,4). Bottom row: DOS at (0,0) (solid line) and (1,1) (dashed line) for three nonmagnetic impurities at $(-1,1)$, $(1,-1)$, and $(-1,-1)$. Pairing symmetry: (a) and (d) $d_{x^2-y^2}$, (b) and (e) $d_{x^2-y^2}+id_{xy}$, and (c) and (f) $d_{x^2-y^2}+is$.

with pure $d_{x^2-y^2}$-wave pairing [Fig. 4(a)]. Similarly, by comparing the LDOS at (1,1) (dashed lines) in Figs. 4(d)–4(f), it is evident that the interfering scatterers can provide a clear distinction between $d+id$ and $d+is$ pairing. Information of the induction of *local* order around the impurities can also be inferred from STM measurements of specific impurity configurations.[17]

We turn now briefly to the study of the classical magnetic impurities in $d_{x^2-y^2}$-wave superconductors. The interference of two magnetic scatterers in an *s*-wave superconductor was

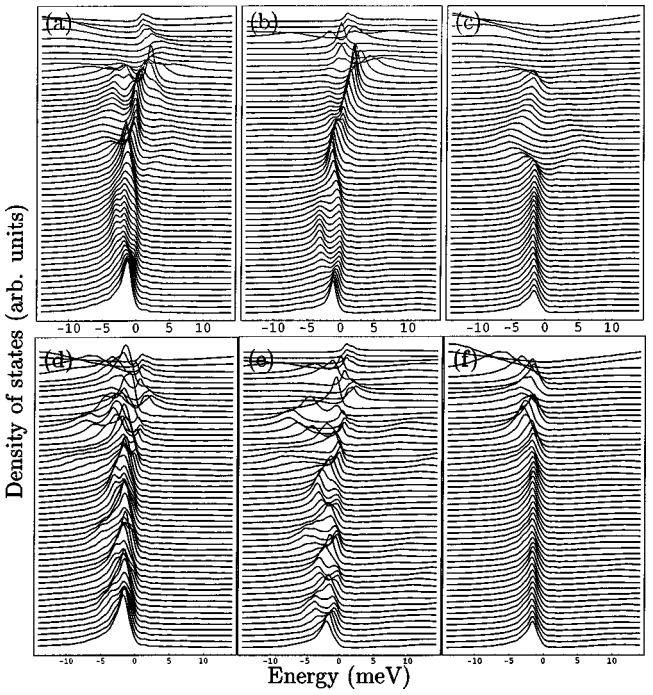

FIG. 5. DOS at (0,0) for (a) and (d) one magnetic and one nonmagnetic impurity, (b) and (e) two magnetic ($V_1^M = V_2^M$), and (c) and (f) two magnetic ($V_1^M = -V_2^M$). The topmost graph in each figure is the DOS when the two scatterers are both positioned at the origin whereas the lowermost shows the DOS at (0,0) and (10,0). Antinodal separation: (a)–(c); nodal separation: (d)–(f).

studied recently by Flatte and Reynolds.[11] For comparison to the nonmagnetic case we use a magnetic potential strength $|V^M| = 700$ meV, which does not, however, model all magnetic impurities (e.g., Ni) on the surface of BSCCO.[3,21] Future experiments will reveal whether the scattering potential formalism utilized here is appropriate or whether more correlated effects are required.[19,20]

Figure 5 shows the quantum interference between two unitary scatterers: Figures 5(a) and 5(d) show one magnetic and one nonmagnetic, Figs. 5(b) and 5(e) two parallel magnetic, and Figs. 5(c) and 5(f) two antiparallal magnetic. In all figures one impurity is fixed below the STM tip at the origin (0,0) while the other is displaced along the [Figs. 5(a)-(-c)] horizontal crystal axis or [Figs. 5(d)–5(f)] along the nodal direction. In Figs. 5(a) and 5(d) it is the nonmagnetic impurity that is fixed at the origin. Again the number of resonances, their position, amplitude, and width depend in detail on the distance and nature of the two scatterers. Further, the spatial evolution of the LDOS is quite similar for Figs. 5(a) and 5(b), and Figs. 5(d) and 5(e). These are, however, very different from the interference between two antiparallel magnetic impurities [Figs. 5(c) and 5(f)] which is dominated by strong destructive interference at small separations along the antinodal direction and a surprisingly fast recovery to the single-impurity case along both the nodal and antinodal directions.

The results presented above remain qualitative since fits to a specific experiment in addition to details from the tunneling matrix elements could also include modified hopping integrals around the impurities, gap suppression, and possibly *both* magnetic and nonmagnetic scattering potentials.[21] We have checked that gap suppression on the bonds around the impurity site does not produce any qualitative changes.[9] However, on a phenomenological level the gap suppression could allow for a competing magnetic order parameter to develop around the impurity. Thus, the gap suppression might be important for explaining the formation of magnetic moments around nonmagnetic impurities as seen by NMR experiments. These issues are currently controversial but the vast amount of information inferred from the quantum interference between multiple impurities may help settle this, and more importantly settle the validity of the scattering potential scenario versus more correlated models.

This work was supported by the Danish Technical Research Council via the Framework Programme on Superconductivity.

[1] A. Yazdani *et al.*, Phys. Rev. Lett. **83**, 176 (1999).
[2] S.H. Pan *et al.*, Nature (London) **403**, 746 (2000).
[3] E.W. Hudson *et al.*, Nature (London) **411**, 920 (2001).
[4] L. Yu, Acta Phys. Sin. **21**, 75 (1965); H. Shiba, Prog. Theor. Phys. **40**, 435 (1968).
[5] A.V. Balatsky, M.I. Salkola, and A. Rosengren, Phys. Rev. B **51**, 15 547 (1995); M.I. Salkola, A.V. Balatsky, and D.J. Scalapino, Phys. Rev. Lett. **77**, 1841 (1996).
[6] D. Morr and N.A. Stavropoulos, Phys. Rev. B **66**, 140508 (2002).
[7] L. Zhu, W.A. Atkinson, and P.J. Hirschfeld, Phys. Rev. B **67**, 094508 (2003).
[8] J.E. Hoffman *et al.*, Science (Washington, DC, U.S.) **297**, 1148 (2002).
[9] Q.-H. Wang and D.-H. Lee, Phys. Rev. B **67**, 020511(R) (2003).
[10] D.J. Derro *et al.*, Phys. Rev. Lett. **88**, 097002 (2002).
[11] M.E. Flatte and D.E. Reynolds, Phys. Rev. B **61**, 14 810 (2000).
[12] D. Morr and N.A. Stavropoulos, Phys. Rev. B **67**, 020502(R) (2003).
[13] Y. Onishi *et al.*, J. Phys. Soc. Jpn. **65**, 675 (1996); U. Michelucci, F. Venturini, and A.P. Kampf, cond-mat/0107621 (unpublished).
[14] J.M. Byers, M.E. Flatte, and D.J. Scalapino, Phys. Rev. Lett. **71**, 3363 (1993).
[15] B.M. Andersen, P. Hedegård, and H. Bruus, Phys. Rev. B **67**, 134528 (2003).
[16] M. Vojta, Y. Zhang, and S. Sachdev, Phys. Rev. Lett. **85**, 4940 (2000); Phys. Rev. B **62**, 6721 (2000).
[17] A.V. Balatsky, Phys. Rev. Lett. **80**, 1972 (1998).
[18] R.B. Laughlin, Phys. Rev. Lett. **80**, 5188 (1998).
[19] Z. Wang and P.A. Lee, Phys. Rev. Lett. **89**, 217002 (2002).
[20] A. Polkovnikov, S. Sachdev, and M. Vojta, Phys. Rev. Lett. **86**, 296 (2001).
[21] M.E. Flatte, Phys. Rev. B **61**, 14 920 (2000); J.-M. Tang and M.E. Flatte, *ibid.* **66**, 060504 (2002).